Spin polarization in valence-band photoemission from non-magnetic (001) surfaces

1997 J. Phys.: Condens. Matter 9 2963

(http://iopscience.iop.org/0953-8984/9/14/011)

J. Phys.: Condens. Matter **9** (1997) 2963–2980. Printed in the UK PII: S0953-8984(97)77134-0

Spin polarization in valence-band photoemission from non-magnetic (001) surfaces

J Henk, T Scheunemann and R Feder

Theoretische Festkörperphysik, Universität Duisburg, D-47048 Duisburg, Germany

Received 13 August 1996

Abstract. For light in a general state of polarization incident off-normally on (001) surfaces of non-magnetic cubic solids, the intensity and spin polarization of photo-electrons in normal emission are investigated. The radiation field inside the solid is approximated firstly by the external field and secondly according to Fresnel's formulae. Analytical expressions are derived to reveal the physical origin of individual spin-polarization components. They also clearly reveal differences between photoemission from surfaces and from single atoms. Quantitative results calculated by a relativistic one-step photoemission formalism are presented for Pt(001). The components of the photo-electron spin-polarization vector are strongly affected by metal optics. In addition to changes in sign and magnitude, components which are identically zero in the external-field approximation can become sizeable as a consequence of the optical response of the solid. Linearly polarized light with the electric field rotated by $\pi/4$ out of the reaction plane induces spin-polarization components comparable to those arising from circularly polarized light.

1. Introduction

Spin–orbit-induced spin polarization of photo-electrons from clean solid surfaces and from ultrathin-film systems is a widespread phenomenon, which in recent years has established itself as a powerful source of detailed information on the electronic structure. For ferromagnetic systems, it combines with the usual exchange-induced spin polarization and is intimately connected with magnetic dichroism, an easily measurable intensity asymmetry upon reversal of the magnetization direction (cf e.g. [1, 2, 3, 4] and references therein). For non-magnetic systems, it occurs 'by itself' and requires for its observation a spin analysis of the photocurrent.

Electron spin polarization (ESP) from non-magnetic surfaces was first found for circularly polarized light (cf e.g. [4, 5, 6] and references therein). This 'optical orientation' is the solid analogue of the Fano effect in atomic photo-ionization (cf e.g. [7]). More recently, linearly polarized light was theoretically and experimentally proven to give rise to three different types of ESP effect in normal emission from non-magnetic surfaces of centrosymmetric crystals. The first of these effects occurs only for surfaces with a threefold rotational axis, e.g. (111) surfaces of cubic solids or (0001) surfaces of hexagonal closely packed solids. S-polarized light induces an in-plane spin-polarization component which can be attributed to the time-reversal degeneracy of Λ_4 and Λ_5 initial states [8, 9]. A second effect is present at all low-index surfaces for off-normally incident p-polarized light. The in-plane spin-polarization component is perpendicular to the reaction plane which is spanned by the light incidence direction and the surface normal [10, 11, 12]. This effect is also produced by unpolarized light [13]. A third effect occurs only at (110) surfaces. S-polarized light

0953-8984/97/142963+18$19.50

produces an ESP component normal to the surface as a consequence of hybridization of initial states with Σ_5^3 and Σ_5^4 spatial symmetry by the spin–orbit interaction [14, 15]. In the following we refer to these spin–orbit-induced phenomena as linear spin-polarization effects (LSPEs).

So far, theoretical photo-electron spin-polarization investigations have focused on geometries of maximal symmetry and—with the exception of some unpublished work [16]—neglected the modification of the radiation field by the optical response of the metal. In particular, the second effect mentioned above [10, 11] was found for p-polarized light incident in a mirror plane normal to the surface. In this paper, we present analytical and numerical investigations of intensity and ESP from non-magnetic surfaces for light in a general state of polarization incident at general polar and azimuthal angles. The approximation of the electric field inside the solid by the external field, which is valid for s-polarized and for normally incident circular polarized light, is now insufficient. A microscopic theory of the optical response being beyond the scope of the present work, we employ the classical field as described by Fresnel's formulae. The light propagation direction inside the solid is then changed and, more importantly, the imaginary part of the dielectric constant induces circular polarized parts of the electric field vector for linear polarized incident light and vice versa.

In the following, we confine ourselves to the case of normal emission. The higher symmetry compared to off-normal emission yields a rich variety of relations between the components of the ESP vector for several set-ups (light incidence angles and polarizations). Further, we focus on (001) surfaces. Since for these the above-mentioned two LSPEs of s-polarized light do not exist, we are dealing with a 'pure' case which allows us to work out the basic symmetry relations. Numerical calculations by means of a relativistic one-step photoemission formalism are performed for Pt(001) with an unreconstructed (1×1) surface, which can actually be produced experimentally [17]. Because of the large atomic number of Pt ($Z = 78$), spin–orbit coupling is strong and so are therefore the ESP effects.

This paper is organized as follows. In section 2 we analytically derive expressions for the intensity and spin polarization of photo-electrons emitted normally from cubic (001) surfaces. To elucidate the general results we focus on some special cases, notably s-, p- and circular polarized light. In section 3 we present and discuss numerical results for Pt(001) for various light polarizations and incidence angles, with an emphasis on the influence of the optical response of the metal within the Fresnel approximation.

2. Analytical details

In the framework of a relativistic golden-rule-type one-step photoemission model, we derive in this section explicit intensity and spin-polarization formulae in normal emission for generally polarized light incident at general polar and azimuthal angles. Some illustrative special cases are discussed in more detail. As a prerequisite for calculating dipole matrix elements, we first outline some essential properties of the initial and final states.

2.1. Symmetry and electronic states

The (001) surfaces of cubic solids show $4mm$ symmetry (C_{4v} in Schönflies notation). We use a Cartesian co-ordinate system with the z-axis along the outward-directed surface normal ([001] direction), the x-axis along [100], and the y-axis along [010]. The basic symmetry operations are the rotation by $\pi/2$ around the surface normal, the reflection at the xz-plane, and the reflection at the plane spanned by the $x = y$-diagonal and the z-axis (cf figure 1).

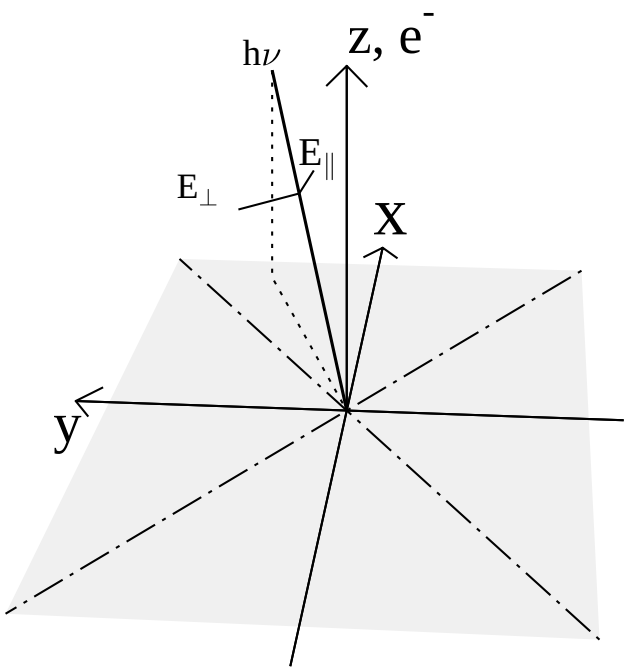

Figure 1. Sketch of the photoemission geometry used in this paper. A cubic (001) surface is indicated by the grey area (xy-plane). The z-axis is along the outward-directed surface normal [001], which is a fourfold rotational axis. The [100] and [010] directions are traces of mirror planes normal to the surface and are labelled x and y, respectively. Dashed lines indicate additional perpendicular mirror planes. The electric field vector of the incident radiation with photon energy $h\nu$ is represented by two orthogonal vectors: within ($E_\parallel$) and perpendicular to ($E_\perp$) the incidence plane which is spanned by the light incidence direction and the surface normal. Electron emission is considered in the z-direction.

Without spin–orbit coupling (SOC), there are five irreducible representations of the point group: four one-dimensional ones (Δ^1, $\Delta^{1'}$, Δ^2, $\Delta^{2'}$) and a two-dimensional one (Δ^5). With SOC included, we have two two-dimensional representations (Δ_6 and Δ_7) of the double group.

Electronic states can be classified with respect to the above representations. Relativistic states, which automatically include SOC, can thus be expressed as

$$|\Delta_6\rangle = |\Delta_6^1\rangle + |\Delta_6^{1'}\rangle + |\Delta_6^5\rangle \tag{1}$$

and

$$|\Delta_7\rangle = |\Delta_7^2\rangle + |\Delta_7^{2'}\rangle + |\Delta_7^5\rangle. \tag{2}$$

The terms on the right side of the above equations have the spatial symmetries of single-group representations as indicated by the superscripts, and each of them consists of a radial part, an angular part, and a Pauli spinor. The latter two follow from group theory (see for example [18]). The radial parts are solutions of the radial Dirac equation. For the present analytical purposes however, we do not compute them, but incorporate them only implicitly into radial matrix elements.

Because of Kramers' degeneracy each electronic state appears in a pair, the wave functions of which have the same radial part and spin-angular parts connected via the

time-reversal operator $\hat{T} = -\mathrm{i}\sigma_y\hat{K}$, where σ_y is the usual Pauli matrix and $\hat{K}$ denotes complex conjugation.

2.2. Photoemission formalism

Details of a fully relativistic one-step theory of photoemission from semi-infinite crystalline systems have been presented in chapter 4.5 of [5]. To obtain transparent analytical expressions, we adopt a golden-rule formulation (neglecting hole lifetime effects) and further approximate the initial- and final-state four-component spinors by two-component spinors $|i_s\rangle$ and $|f_s\rangle$, with $s = \pm$, which are the time-reversal degenerate pair eigenfunctions of a Pauli-like Hamiltonian including spin–orbit coupling (see [5], p 131). The photocurrent at the detector is then described by a 2×2 spin density matrix ϱ with elements

$$\varrho_{ss'}(E_f) = \sum_{i,s''} \langle f_s|H'|i_{s''}\rangle\langle i_{s''}|H'|f_{s'}\rangle\ \delta(E_f - \hbar\omega - E_{i_{s''}}) \tag{3}$$

where H' is the electron–photon interaction, to be discussed in more detail below. The final states $|f_+\rangle$ and $|f_-\rangle$ both have the energy E_f, and only initial states with energy $E_f - \hbar\omega$ contribute, with $\hbar\omega$ denoting the photon energy. As a consequence of lattice periodicity parallel to the surface, all states have the same surface-parallel wave vector $\boldsymbol{k}_\parallel$, which is fixed by E_f and the detection direction. For normal emission, which is considered in this paper, $\boldsymbol{k}_\parallel = \boldsymbol{0}$, the final states $|f_s\rangle$ have the totally symmetric Δ_6 form (cf equation (1)) and the initial states $|i_s\rangle$ are of Δ_6 or Δ_7 symmetry (cf equations (1) and (2)).

The intensity I and the electron spin polarization $\boldsymbol{P}$ are obtained from ϱ as

$$I = \mathrm{tr}(\varrho) \qquad \boldsymbol{P} = \mathrm{tr}(\boldsymbol{\sigma}\,\varrho)/I \tag{4}$$

with the vector $\boldsymbol{\sigma}$ comprising the three Pauli matrices.

For valence-band photoemission by radiation in the vacuum-ultraviolet (VUV) regime and below, it is adequate to approximate the photon–electron interaction H' by the dipole length form $\boldsymbol{E}\cdot\boldsymbol{r}$, where $\boldsymbol{E}$ is the electric vector of the radiation field inside the solid, assumed to be spatially constant. The light polarization can be characterized by the two quantities $E_\parallel$ and $E_\perp$ (see figure 1), which are the amplitudes of the components of $\boldsymbol{E}$ parallel and perpendicular to the plane of incidence, respectively. In the usual terminology of classical optics, s-polarized light (from German 'senkrecht', i.e. perpendicular) is thus described by $(E_\parallel, E_\perp) = (0, 1)$, and p-polarized light (from 'parallel') by $(E_\parallel, E_\perp) = (1, 0)$, where 'perpendicular' and 'parallel' also refer to the plane of incidence. For circularly polarized light, there is a phase shift of $\pm\mathrm{i}$ between the s- and p-components of $\boldsymbol{E}$, i.e. $(E_\parallel, E_\perp) = (1, \pm\mathrm{i})/\sqrt{2}$. Further, we will consider below the particularly interesting special case of linearly polarized light $(E_\parallel, E_\perp) = (1, \pm1)/\sqrt{2}$, which for short we will refer to as sp-polarized light.

In the following, we approximate the radiation field inside the solid macroscopically according to classical electrodynamics (cf e.g. [19]). We recall that the dielectric constant ϵ' of the solid is in general complex and related to the refractive index n' by $n' = \sqrt{\epsilon'}$ where n' has a positive real part. (In the following, quantities inside the solid are indicated by a prime.) The internal polar angle ϑ' is related to the external one (vacuum side) by Snell's law,

$$\sin\vartheta' = \sin\vartheta/n' \tag{5a}$$

$$\cos\vartheta' = -\sqrt{\epsilon' - \sin^2\vartheta}/n'. \tag{5b}$$

Because ϵ' is complex, ϑ' is also necessarily complex. The internal amplitudes of the electric field are given by Fresnel's formulae as

$$E'_\perp = \frac{2\cos\vartheta\, E_\perp}{\cos\vartheta + \sqrt{\epsilon' - \sin^2\vartheta}} \tag{6a}$$

$$E'_\parallel = \frac{2n'\cos\vartheta\, E_\parallel}{\epsilon'\cos\vartheta + \sqrt{\epsilon' - \sin^2\vartheta}} \tag{6b}$$

which are also complex due to ϵ'. Note that incident s- and p-polarized light remain so inside the solid, whereas for general linear polarized light and for circular polarized light the internal field becomes elliptically polarized.

We now evaluate, for normal emission, the matrix elements in equation (3) with the initial states according to equations (1) and (2) and the final state according to equation (1). This leads firstly to an explicit dependence on the incidence angles of the light (polar angle ϑ and azimuth φ) and on the light polarization (given by $E_\parallel$ and $E_\perp$). Secondly, there remain partial radial transition matrix elements $M_j^{(i\to k)}$, where i indicates the spatial symmetry part of the initial state with double-group symmetry $j = 6, 7$, and $k = 1, 5$ the spatial symmetry part of the final state (which necessarily has double-group symmetry Δ_6). It turns out that these matrix elements occur pairwise such that they can be combined into elements $M_j^{(i)}$ defined as

$$M_6^{(1)} = M_6^{(1\to 1)} + M_6^{(5\to 5)} \tag{7a}$$

$$M_6^{(5)} = M_6^{(5\to 1)} + M_6^{(1\to 5)} \tag{7b}$$

$$M_7^{(5)} = M_7^{(5\to 1)} + M_7^{(2\to 5)}. \tag{7c}$$

If spin–orbit coupling in the final state is comparatively weak, as is often the case, the index i in $M_j^{(i)}$ reflects mainly the spatial symmetry type of the relevant initial-state part. The expression for the density matrix ϱ, which is thus eventually obtained, is in general a sum of two terms, one arising from Δ_6 and the other from Δ_7 initial states. Consequently, the total photocurrent is the sum of the two corresponding individual photocurrents, $I = I_6 + I_7$, and the total ESP is

$$\boldsymbol{P} = \frac{\boldsymbol{P}_6 I_6 + \boldsymbol{P}_7 I_7}{I_6 + I_7}. \tag{8}$$

2.3. General photocurrent and polarization expressions

Bearing the above decomposition in mind, we present in the following separately the explicit results obtained for Δ_6 and for Δ_7 initial states. Although somewhat complicated at first sight, these expressions have a simple structure: products of partial radial matrix elements multiplied by terms involving the electric field components and angles.

From Δ_6 initial states (cf equation (1)) we obtain the photoemission intensity

$$I_6 = 2|M_6^{(1)}|^2\,|\sin\vartheta' E'_\parallel|^2 + 2|M_6^{(5)}|^2\left(|E'_\perp|^2 + |\cos\vartheta' E'_\parallel|^2\right) \tag{9}$$

where the radial matrix elements $M_6^{(i)}$ are defined according to equation (7). SOC in the final state is thus included. However, since it is often relatively weak, we prefer to ignore it in the following discussions. First, we note that I_6 is independent of the azimuth φ. Further, emission from states with Δ^5 spatial symmetry (second term in equation (9)) is mediated by the surface in-plane components of the electric field vector. The component of $\boldsymbol{E}$ normal to the surface leads to emission from states with Δ^1 spatial symmetry (first term in equation (9)).

The in-plane components of the ESP vector $\boldsymbol{P}$ read

$$P_{6x} = \frac{-4}{I_6}\Big\{\mathrm{Im}(M_6^{(1)}M_6^{(5)\star})\big[\cos\varphi\ \mathrm{Re}(\sin\vartheta' E'_\parallel E'^{\star}_\perp) + \sin\varphi\ \mathrm{Re}(\sin\vartheta'\cos\vartheta'^{\star})|E'_\parallel|^2\big] + \mathrm{Re}(M_6^{(1)}M_6^{(5)\star})\big[\cos\varphi\ \mathrm{Im}(\sin\vartheta' E'_\parallel E'^{\star}_\perp) + \sin\varphi\ \mathrm{Im}(\sin\vartheta'\cos\vartheta'^{\star})|E'_\parallel|^2\big]\Big\} \tag{10a}$$

$$P_{6y} = \frac{-4}{I_6}\Big\{\mathrm{Im}(M_6^{(1)}M_6^{(5)\star})\big[\sin\varphi\ \mathrm{Re}(\sin\vartheta' E'_\parallel E'^{\star}_\perp) - \cos\varphi\ \mathrm{Re}(\sin\vartheta'\cos\vartheta'^{\star})|E'_\parallel|^2\big] + \mathrm{Re}(M_6^{(1)}M_6^{(5)\star})\big[\sin\varphi\ \mathrm{Im}(\sin\vartheta' E'_\parallel E'^{\star}_\perp) - \cos\varphi\ \mathrm{Im}(\sin\vartheta'\cos\vartheta'^{\star})|E'_\parallel|^2\big]\Big\}. \tag{10b}$$

The products of matrix elements involving initial-state parts with Δ^1 and Δ^5 spatial symmetry directly reflect the spin–orbit-coupling origin of P_{6x} and P_{6y}: without hybridization of the two spatial symmetry parts by SOC, these products would not occur. Further, there is a delicate dependence on the phase of the matrix elements and of the light polarization. The normal component is

$$P_{6z} = \frac{-4}{I_6}|M_6^{(5)}|^2\,\mathrm{Im}(\cos\vartheta' E'_\parallel E'^{\star}_\perp). \tag{11}$$

For Δ_7 initial states (cf equation (2)), there are only matrix elements involving the Δ^5 part, and we obtain

$$I_7 = 2|M_7^{(5)}|^2\left(|E'_\perp|^2 + |\cos\vartheta'|^2|E'_\parallel|^2\right) \tag{12}$$

and the ESP shows only a non-zero normal component,

$$P_{7z} = \frac{4}{I_7}|M_7^{(5)}|^2\,\mathrm{Im}(\cos\vartheta' E'_\parallel E'^{\star}_\perp). \tag{13}$$

The ESP components normal to the surface, P_{6z} and P_{7z}, are seen to involve only the Δ_6^5 spatial symmetry parts of the initial-state wave functions.

For the discussion of the above expression we proceed as follows. We first neglect the optical response of the solid and consider in some detail the results for typical special cases of light polarization. Subsequently, we focus on effects brought about by the optical response.

2.4. Special cases in the absence of optical response

In this section, we discuss intensity and spin-polarization results, which one obtains if the internal radiation field is simply approximated by the external field. Obviously, these results correspond to $\epsilon' = 1$ and follow from our above general equations by replacing the primed incidence angle and electric field components by their un-primed (external) counterparts. Firstly they are approximations for systems and photon energies with ϵ' close to unity, secondly we find them rather interesting in their own right, and thirdly they provide a reference basis for the subsequent elaboration of effects produced by the optical response.

2.4.1. Linear polarized light. For off-normally incident p-polarized light, i.e. $(E_\parallel, E_\perp) = (1, 0)$, the intensity expression equations (9) and (12) become

$$I_6 = 2\left(|M_6^{(1)}|^2\sin^2\vartheta + |M_6^{(5)}|^2\cos^2\vartheta\right) \tag{14a}$$

$$I_7 = 2|M_7^{(5)}|^2\cos^2\vartheta. \tag{14b}$$

The ESP for Δ_7 initial states (cf equation (13)) is now identically zero. For Δ_6 states, equations (10*b*) and (11) reduce to

$$P_{6x} = -2\sin 2\vartheta \sin\varphi \,\mathrm{Im}(M_6^{(1)} M_6^{(5)\star})/I_6 \tag{15a}$$

$$P_{6y} = 2\sin 2\vartheta \cos\varphi \,\mathrm{Im}(M_6^{(1)} M_6^{(5)\star})/I_6 \tag{15b}$$

$$P_{6z} = 0. \tag{15c}$$

The spin-polarization vector $\boldsymbol{P}$ is normal to the plane of incidence and its modulus does not depend on the azimuth φ. It vanishes for normal incidence ($\vartheta = 0^\circ$) and for grazing incidence ($\vartheta = 90^\circ$). The origin of this LSPE is the hybridization of initial states with Δ^1 and Δ^5 spatial symmetry due to SOC: without SOC no products of matrix elements of initial-state parts with different spatial symmetry would occur. Thus, there would be no ESP. This LSPE has been theoretically predicted by Tamura and Feder [10, 11] and experimentally confirmed by Schmiedeskamp *et al* [12]. It is also present in photoemission from (111) and (110) surfaces. For ferromagnetic systems, it gives rise to magnetic linear dichroism in angular distribution (MLDAD) in the standard geometry (plane of incidence normal to the in-plane magnetization) [20].

The results for s-polarized light can be obtained from the above by setting $\vartheta = 0^\circ$, i.e. normal incidence, or, equivalently, from the general expressions in subsection 2.3 by setting $(E_\parallel, E_\perp) = (0, 1)$. In particular, the ESP is then identically zero.

A particularly interesting special case of off-normally incident linear polarized light is one with the electric field rotated by $\pi/4$ out of the plane of incidence, i.e. $(E_\parallel, E_\perp) = (1, \pm 1)/\sqrt{2}$, which in the following we refer to as sp-polarized light. As will be seen below, this case is closely connected to that of off-normally incident circular polarized light. For the intensities we obtain

$$I_6 = \sin^2\vartheta |M_6^{(1)}|^2 + (1 + \cos^2\vartheta)|M_6^{(5)}|^2 \tag{16a}$$

$$I_7 = (1 + \cos^2\vartheta)|M_7^{(5)}|^2 \tag{16b}$$

and the ESP reads

$$P_{6x} = [\mp 2\sin\vartheta\cos\varphi - \sin 2\vartheta \sin\varphi]\,\mathrm{Im}(M_6^{(1)} M_6^{(5)\star})/I_6 \tag{17a}$$

$$P_{6y} = [\mp 2\sin\vartheta\sin\varphi + \sin 2\vartheta \cos\varphi]\,\mathrm{Im}(M_6^{(1)} M_6^{(5)\star})/I_6 \tag{17b}$$

$$P_{6z} = 0 \tag{17c}$$

and $\boldsymbol{P}_7 = 0$. Consider especially the case $\varphi = 0^\circ$, i.e. light incident in the xz-plane. P_{6y} is then seen to have the same numerator as above for off-normal incident p-polarized light, but I_6 in the denominator is somewhat different. A more striking difference is that for sp-polarized light P_{6x} does not vanish. By switching the light polarization from $(E_\parallel, E_\perp)$ to $(E_\parallel, -E_\perp)$, one reverses the sign of P_x, whereas P_y remains unchanged.

2.4.2. Circular polarized light. For left- and right-handed circular polarized light we have a phase shift $\pm$i between the s- and p-polarized partial waves of $\boldsymbol{E}$, i.e. $(E_\parallel, E_\perp) = (1, \pm\mathrm{i})/\sqrt{2}$. Let us first consider the case of normal incidence, $\vartheta = 0^\circ$. The intensities read

$$I_6 = 2|M_6^{(5)}|^2 \qquad I_7 = 2|M_7^{(5)}|^2 \tag{18}$$

i.e. they are the same as for s-polarized light. The in-plane components of the ESP vanish and P_z becomes

$$P_{6z} = \pm 2|M_6^{(5)}|^2/I_6 = \pm 1 \tag{19a}$$

$$P_{7z} = \mp 2|M_7^{(5)}|^2/I_7 = \mp 1. \tag{19b}$$

$\boldsymbol{P}$ is thus normal to the surface and aligned to the photon helicity, which corresponds to the so-called complete optical orientation. Further, the partial polarizations are complete and the sign of P_{6z} is opposite to that of P_{7z}.

We use the term 'complete optical orientation' in the sense that the ESP vector is parallel or antiparallel to the light helicity. Further, the term 'optical orientation' is restricted to the case that an ESP component is only present if there is a non-zero phase shift between $E_\parallel$ and $E_\perp$, as is the case for circular polarized light. 'Optical orientation' is thus a special case of photo-electron spin polarization from (non-magnetic) solids.

For off-normal incidence we arrive at

$$I_6 = \sin^2\vartheta\,|M_6^{(1)}|^2 + (1+\cos^2\vartheta)|M_6^{(5)}|^2 \tag{20a}$$

$$I_7 = (1+\cos^2\vartheta)|M_7^{(5)}|^2 \tag{20b}$$

and

$$P_{6x} = \left[\pm 2\sin\vartheta\cos\varphi\,\mathrm{Re}(M_6^{(1)}M_6^{(5)\star}) - \sin 2\vartheta\sin\varphi\;\mathrm{Im}(M_6^{(1)}M_6^{(5)\star})\right]/I_6 \tag{21a}$$

$$P_{6y} = \left[\pm 2\sin\vartheta\sin\varphi\,\mathrm{Re}(M_6^{(1)}M_6^{(5)\star}) + \sin 2\vartheta\cos\varphi\;\mathrm{Im}(M_6^{(1)}M_6^{(5)\star})\right]/I_6 \tag{21b}$$

$$P_{6z} = \pm 2\cos\vartheta\,|M_6^{(5)}|^2/I_6. \tag{21c}$$

The in-plane components of $\boldsymbol{P}_7$ vanish and the normal component is

$$P_{7z} = \mp 2\cos\vartheta\,|M_7^{(5)}|^2/I_7. \tag{22}$$

The modulus of $\boldsymbol{P}_6$ is independent of φ. Further, if the incidence plane is rotated by $\delta\varphi$ around the surface normal, $\boldsymbol{P}$ is rotated by the same angle. The in-plane components of $\boldsymbol{P}$ are sums of two terms. The first term can be attributed to 'optical orientation' because it depends on $\sin\vartheta$ and changes sign if the helicity is reversed. The second term depends on $\sin 2\vartheta$ and is seen to be identical to the LSPE term for off-normal incident p-polarized light. The two types of in-surface-plane polarization are perpendicular to each other, as is evident from the trigonometrical factors with φ. For the special azimuth $\varphi = 0^\circ$, the first and second terms by themselves produce P_{6x} and P_{6y}, respectively. Upon reversal of the light helicity, P_{6x} and P_{6z} then change sign, whereas P_{6y} does not.

From the above expressions it is clear that in general $\boldsymbol{P}$ is not aligned to the incidence direction, i.e. there is no complete optical orientation. If it were so, there would be no component of $\boldsymbol{P}$ perpendicular to the plane of incidence. Further, P_z and the remaining in-plane component would be identical, except for geometrical factors which correct for the polar angle of incidence. Complete optical orientation occurs only for normal incidence ($\vartheta = 0^\circ$) and grazing incidence ($\vartheta = 90^\circ$), i.e. where there is no LSPE for off-normal incident p-polarized light.

The deviation of the direction of $\boldsymbol{P}$ from the incidence direction of the circular polarized light depends distinctly on the symmetry type of the initial state. For Δ_7 initial states, $\boldsymbol{P}$ is always perpendicular to the surface, irrespective of the angle of the incidence direction. For Δ_6 initial states (cf equation (21)), $\boldsymbol{P}$ has in general, in addition to P_{6z}, two non-vanishing components parallel to the surface, i.e. in particular a component normal to the incidence plane. P_{6x} and P_{6y} arise from the spin–orbit hybridization of initial states with Δ^1 and Δ^5 spatial symmetry, whereas P_{6z} depends only on initial states with Δ^5 spatial symmetry.

Comparing these results with the above ones for sp-polarized light, the main distinction is that for circular polarized light there is a non-vanishing P_z, i.e. there is 'optical orientation'. Further, there is a difference in the component parallel to the surface and to the incidence plane (P_{6x} in the case $\varphi = 0^\circ$): for circular polarized light it is proportional to $\mathrm{Re}(M_6^{(1)}M_6^{(5)\star})$, for sp-polarized light it is proportional to $\mathrm{Im}(M_6^{(1)}M_6^{(5)\star})$. Therefore, by

measuring P_x for these two different light polarizations one is able to determine products of matrix elements and their phase directly. This implies new information on the electronic states. From the experimental point of view, the set-up can be left unchanged and only the light polarization has to be switched from 'sp' to 'circular'.

2.5. Influence of the optical response

We now focus on effects which arise from approximating the internal radiation field according to Fresnel rather than simply replacing it by the external field.

Perhaps the most striking effect is that the optical response can produce components of $\boldsymbol{P}$ which are identically zero in its absence. Consider for example linearly polarized light, for which both $E_\parallel$ and $E_\perp$ is real (and non-zero) outside the solid. In the external-field approximation, P_{6z} and P_{7z} are zero because the imaginary parts in equations (11) and (13) vanish. With Fresnel's correction, however, they will in general be non-zero, since $E_\perp$ and $E_\parallel$ (cf equations (6)) are complex, with a relative phase shift between them, and furthermore $\cos\vartheta$ (cf equation (5*b*)) is complex. These three factors are obviously complex if ϵ is complex or if it is real and smaller than $\sin^2\vartheta$. The resulting P_{6z} and P_{7z} versus initial state energy spectra will have the same shape as for circular polarized incident light because only the transition matrix elements depend on the initial-state energy. For the special case of s-polarized incident light, $\boldsymbol{P}$ remains identically zero and the intensity spectra are scaled by a factor $|E'_\perp|^2$ (cf equation (6*b*)). For p-polarized light, $\boldsymbol{P}_7$ and P_{6z} remain identically zero, I_7 spectra are scaled by a factor, and I_6, P_{6x}, and P_{6y} spectra are generally modified with respect to their counterparts without optical response (cf equations (9), (10), and (11)).

Another consequence of the optical response is a change in the dependence of both the intensity and the ESP on ϑ. This is most obvious in the limit of grazing incidence ($\vartheta = 90^\circ$). Employing the external field and angle in equations (9) and (12) gives in general a finite photocurrent. In contrast, the photocurrent vanishes in the Fresnel approximation, since according to equations (6) the electric field inside the solid is zero. The ϑ-dependence is easily computed from our analytical expressions, taking in the Fresnel case the internal angle and field parts as obtained from equations (5) and (6) with the experimental dielectric constant $\epsilon = -0.23 + \mathrm{i}2.16$ for Pt at $h\nu = 21.2$ eV [21].

The I_7 curves calculated for various light polarizations are shown in figure 2. Note that they are identical for circular polarized light and for linear polarized light with the electric field vector rotated by an angle $\alpha = \pi/4$ out of the incidence plane, which for short we refer to as sp-polarized light. Likewise, P_{6z} and P_{7z} (cf equations (11) and (13)) are strongly affected by the optical response. For circular polarized light, in the external-field approximation, the denominators remain finite in the limit $\vartheta = 90^\circ$ and the $\cos\vartheta$ term in the numerators lets the polarizations vanish. 'With Fresnel', however, the denominators also go to zero, resulting in non-zero polarizations at $\vartheta = 90^\circ$. The computed $P_{7z}(\vartheta)$ curves are shown in figure 2. The influence of the Fresnel correction is seen to be strongest at polar angles larger than 60°. For sp-polarized light, the effect of the optical response on P_{7z} is even more drastic: whilst identically zero in the external-field approximation, P_{7z} acquires large values in the Fresnel-field approximation, as can be seen in figure 2. Its sign is opposite to that for circular polarized light. The sign of P_{7z} obviously changes if $E_\perp$ is replaced by $-E_\perp$, i.e. going to negative helicity for circular polarized light and to $\alpha = -\pi/4$ for linear polarized light.

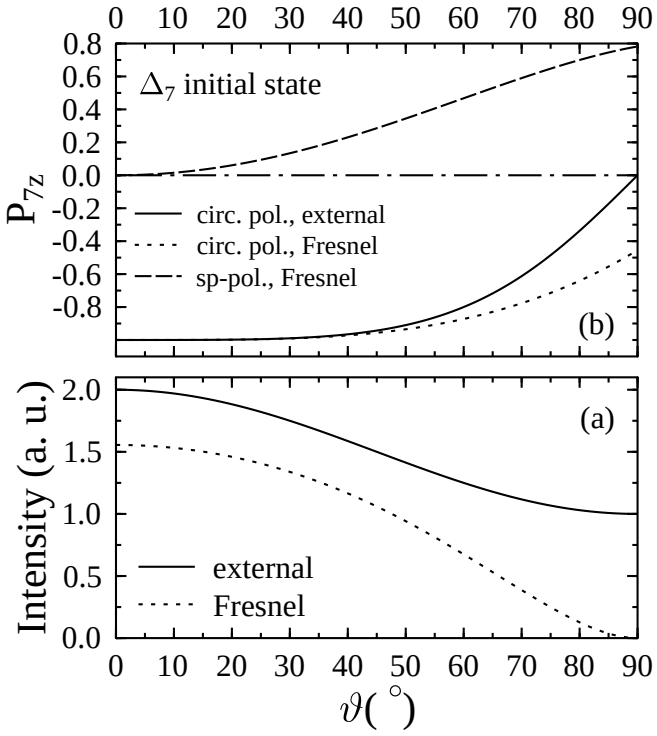

Figure 2. Photoemission intensity (a) and spin polarization component P_z normal to the surface (b) from Δ_7 initial states for positive-helicity circular and for linear sp-polarized radiation as functions of the polar incidence angle ϑ, computed from the analytical expressions equations (12) and (13). Solid (short-dashed) lines: for circular polarized light with the internal electric field taken as the external field (Fresnel field, for dielectric constant value $-0.23 + \mathrm{i}2.16$ of Pt at 21.22 eV photon energy). For sp-polarized light, the intensities are the same, and P_{7z} is non-zero only in the Fresnel case (long-dashed line).

2.6. Comparison with photoemission from atoms

Comparison of the above results with those for spin polarization in photoemission from a single atom reveals some corresponding facts, but also pronounced differences which can be attributed to the presence of the solid surface, i.e. to a reduction of symmetry with respect to the atomic case.

Consider light incident along the $z^{(\mathrm{at})}$ axis on an unpolarized atom. (We indicate the co-ordinates used in the atomic case with the superscript (at) to distinguish them from those of the solid surface case). Electrons are detected at a polar angle $\vartheta^{(\mathrm{at})}$ with respect to the $z^{(\mathrm{at})}$ axis. The reaction plane is spanned by these directions, see figure 3 (cf also table 5.1 in [7]). The components of the electron spin polarization are $P_z^{(\mathrm{at})}$ (along the light incidence axis), $P_p^{(\mathrm{at})}$ (parallel to the reaction plane and perpendicular to the $z^{(\mathrm{at})}$ axis), and $P_n^{(\mathrm{at})}$ (normal to the reaction plane).

We first discuss optical orientation by circular polarized light. For an atom there is complete alignment of electron spin and helicity, i.e. only $P_z^{(\mathrm{at})}$ is non-zero, if the angle between incidence direction and detection direction is 0°, 90° or 180° which follows immediately from symmetry. For example, for 0° or 180° a rotation about any angle

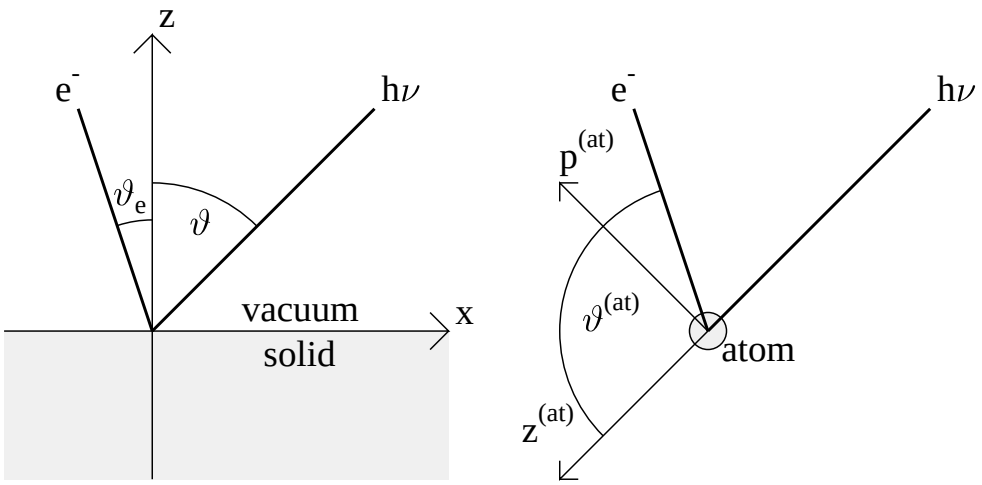

Figure 3. Geometry of photoemission from a solid surface (left) and an atom (right). Photons impinge from the first quadrant ($h\nu$) onto the surface of the solid (grey rectangle) or onto the atom (grey circle). Electrons are detected in the second quadrant (e^-). The surface normal is marked z, the in-plane axis x. The y-axis points into the plane of the drawing. In the left panel, ϑ_e denotes the polar angle of electron emission. In the atomic case, the light incidence direction is labelled $z^{(at)}$, the axis perpendicular $p^{(at)}$. The axis perpendicular to the drawing plane is $n^{(at)}$.

around the emission direction ($z^{(at)}$) is a symmetry operation which leaves only $\boldsymbol{P}$ along this axis invariant (in this case the symmetry group is $C_{\infty v}$). In the case of 90°, reflection at the plane perpendicular to the incidence direction is a symmetry operation. Thus the in-plane components of $\boldsymbol{P}$ are zero, leaving only the perpendicular component non-zero. For any other angle, all Cartesian components of $\boldsymbol{P}$ are allowed to be non-zero. In particular, $P_n^{(at)}$ does not change sign if the helicity of the light is reversed, as in the case of emission from a solid.

For p-polarized light only $P_n^{(at)}$ is non-zero and depends on $\sin 2\vartheta^{(at)}$. Further, this component is brought about by the same transition matrix elements as in the case of circular polarized light.

In order to compare the atomic case with the solid surface case, one has to consider the surface plane explicitly (see figure 3). Let us start with the case of complete alignment, e.g. circular polarized light and $\vartheta^{(at)} = 180°$ (there is no case which corresponds to $\vartheta^{(at)} = 0°$ because valence-band photoemission from solid surfaces cannot be performed in transmission due to the small mean free path of the photo-electrons). In normal emission from the solid surface, complete alignment is observed in normal and grazing incidence. Thus, we find a close correspondence to the atomic case. However, the surface plane breaks the symmetry of the system in the sense that off-normal emission and off-normal incidence with 0° and 90° between incidence and detection direction yield no complete alignment (which can be attributed to the LSPE for p-polarized light). We checked this result by numerical calculations for Pt(001).

In the case of arbitrary $\vartheta^{(at)}$ we have $P_n^{(at)}$ non-zero. This case corresponds to off-normally incident circular polarized light which also produces a $\boldsymbol{P}$-component perpendicular to the reaction plane. This component is due to the LSPE for p-polarized light. In the two cases, the angular dependence is $\sin 2\vartheta^{(at)}$ or $\sin 2\vartheta$, respectively. Further, in both cases

the $\boldsymbol{P}$-components are brought about by transition matrix elements which differ from those which produce the other ESP components. In conclusion, we find an additional close correspondence between the atomic and the solid surface case.

3. Numerical results for Pt(001)

The analytical expressions presented in section 2 show which spin-polarization components can occur and reveal details of their physical origin. To determine their magnitude and spectral shape, we have, for an unreconstructed (001) surface of Pt (with $Z = 78$ and consequently large SOC), performed numerical calculations by means of a fully relativistic one-step-model Green function theory of photoemission [22]. For the purpose of interpreting the resulting spectra, we have simultaneously calculated the relativistic bulk band structure along the Δ line. As the effective quasi-particle potentials for initial and final states, we employed the same as in earlier calculations for Pt(111) [23] and Pt(110) [14]. In the following, we present some typical results obtained for linear and circular polarized 21.22 eV (He_I) photons incident at $\vartheta = 45^\circ$ in the xz-plane ($\varphi = 0^\circ$). For the internal radiation field in the Fresnel approximation we used the experimentally determined dielectric constant $\epsilon = -0.23 + i2.16$ [21], which differs strongly from the vacuum value and in particular has a large imaginary part.

3.1. Band structure and photoemission by p-polarized light

As a basis for interpreting our calculated photoemission intensity and spin-polarization spectra, we show in panel (a) of figure 4 the relativistic bulk band structure of Pt along the Γ–Δ–X line for the initial states and—shifted downward by the photon energy—for the final states. Crossing points between initial- and final-state bands then mark energies at which direct bulk interband transitions are possible. The photoemission intensity spectra (as obtained by our one-step-model Green function calculations) for p-polarized light at several polar incidence angles ϑ are seen (panel (b) of figure 4) to have their maxima at such crossing point energies, i.e. can be interpreted in terms of direct transitions. The dependence of the spectra on ϑ is readily understood from the selection rule findings that emission from initial-state parts with Δ^1 (Δ^5) spatial symmetry is mediated by the component of the electric field normal (parallel) to the surface. For example, the peak at -0.5 eV is maximal for normal incidence (i.e. $\boldsymbol{E}$ parallel to the surface) and absent for grazing incidence (i.e. $\boldsymbol{E}$ normal to the surface). It can be traced to a transition from a Δ_7 initial state, which has a significant Δ^5 spatial symmetry part. Converse behaviour with ϑ is observed for the main peak at -1.8 eV, which stems from Δ_6 initial states with substantial Δ^1 spatial symmetry parts.

For p-polarized light incident at $\vartheta = 45^\circ$, the intensity changes due to employing the Fresnel field instead of the external field are shown in panel (c) of figure 4. Firstly, there is a significant reduction of the overall intensity which is due to the reduction of the modulus of the electric field vector inside the solid with respect to its vacuum value by a factor of about 0.77. Further, the ratio between the maxima at -1.8 eV and -0.8 eV is strongly decreased. This can be explained by the change of the light propagation direction from polar angle 45° to about 17°, the real part of the complex internal angle as given by Snell's law. The electric field component normal (parallel) to the surface is thus reduced (enhanced), leading to a decrease (increase) of emission from initial-state parts of Δ^1 (Δ^5) spatial symmetry, as has been demonstrated in panel (b).

In line with our analytical results, the numerical calculations yield a photo-electron spin polarization vector normal to the reaction plane, i.e. in the present geometry only a

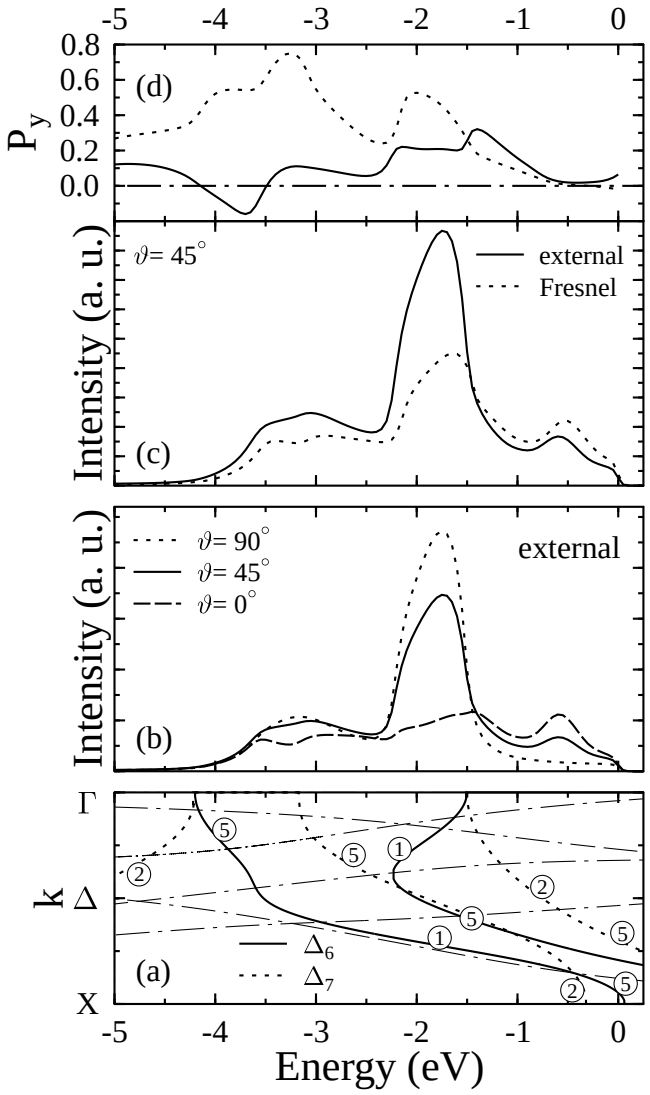

Figure 4. Normal photoemission from Pt(001) by p-polarized 21.22 eV light incident at polar angle ϑ in the xz-plane. (a) Symmetry-resolved band structure along [001] (z-axis, Γ–Δ–X). Initial states are classified with respect to their double-group symmetry (Δ_6 solid and Δ_7 dotted). The prominent spatial symmetry in various parts of the initial-state bands is indicated by encircled numbers. Final-state bands with prominent Δ^1 spatial symmetry are shifted down by the photon energy (dash–dotted). (b) Photoemission intensity in the external-field approximation: for $\vartheta = 90^\circ$ (grazing incidence, dotted), $\vartheta = 45^\circ$ (solid), and $\vartheta = 0^\circ$ (normal incidence, dashed). Note that the latter spectrum is the same as for s-polarized light. (c) Photoemission intensity for incidence at $\vartheta = 45^\circ$ calculated with the external electric field (solid) and the Fresnel field (dotted). (d) Photo-electron spin polarization component P_y along [010] (y-axis). Line styles are as in panel (c). (The components P_x and P_z are identically zero.)

non-vanishing component P_y, which we show in panel (d) of figure 4. It exhibits large features (up to 70%), several of which coincide in energy with sizeable intensity values. The effect of employing the Fresnel field is very strong around -2 eV and between -3 eV

and -4 eV. We recall from our analytical results that in the external-field approximation, P_y is brought about by $\mathrm{Im}(M_6^{(1)}M_6^{(5)\star})$ (cf equation (15*b*)). In the Fresnel approximation, in which in the present geometry $E_\parallel$ is complex, there is (cf equation (10*b*)) an additional term which is proportional to $\mathrm{Re}(M_6^{(1)}M_6^{(5)\star})$. The difference between the spin-resolved intensities (not shown here) is largest where emission from $\Delta_6^1\Delta_6^5$ hybrids is strong. This allows the identification of such spin–orbit-induced hybridization regions in reciprocal space. On the other hand, P_y vanishes for emission from initial states of almost pure spatial symmetry. This is illustrated in figure 4 around -0.5 eV, where transition from an initial state of Δ^5 spatial symmetry produces an intensity peak, but the spin polarization (with and without Fresnel) vanishes.

3.2. Photoemission by sp-polarized light

If the electric field vector of incident linear polarized light is rotated by some angle, in particular $\pi/4$, out of the plane of incidence (i.e. 'sp-polarized' light), normal photoemission results are modified in a number of respects, some of which are quite drastic. We demonstrate this in the left-hand part of figure 5.

The intensity spectra (bottom panel) are similar to those for p-polarized light (cf figure 4), but emission from Δ^5 (Δ^1) initial-state parts is enhanced (reduced) since sp-polarized light has a larger (smaller) projection of $\boldsymbol{E}$ parallel (normal) to the surface. The P_y spectra are similar in shape to those for p-polarized light, but reduced in magnitude and different in some details (notably the height of the maximum at -1.5 eV relative to its neighbours). This can easily be understood from our analytical expressions in section 2. As suggested by (10*a*) and (17*a*), there is now also a polarization component P_x, which attains sizeable values. In the external-field approximation, $P_x(E)$ is seen to have the same shape as $-P_y(E)$, but is larger by a factor $\sqrt{2}$. This is also obvious from equation (17*a*).

The influence of crystal optics (i.e. employing the Fresnel field) on I and $P_y(E)$ is very similar as in the case of p-polarized light, which we discussed in subsection 3.1. This similarity extends to $P_x(E)$. A qualitatively new effect is however the appearance of P_z (normal to the surface) (cf top left-hand panel of figure 5), which reaches values up to 25%. As can be seen from equation (11), P_z requires for its existence a phase difference between $E_\parallel$ and $E_\perp$. Such phase difference is brought about by the imaginary part of the dielectric constant. Especially for $\epsilon = -0.23 + \mathrm{i}2.16$ (for Pt at $h\nu = 21.22$ eV) and sp-polarized light incident at $\vartheta = 45^\circ$, one obtains from Fresnel's formulae $E'_\parallel = (0.65 - \mathrm{i}0.34)/\sqrt{2}$ and $E'_\perp = (0.58 - \mathrm{i}0.43)/\sqrt{2}$. Since one may view this internal field as composed of a circular and a linear polarized part, and since a linear polarized (internal) field cannot produce P_z, the spectral shape of $P_z(E)$ should be similar as for circular polarized incident light (provided the latter retains a circular polarized part inside the solid). This is indeed the case, as can be seen by comparison with the top panel of the right-hand part of figure 5. With regard to the opposite sign we recall that $P_z^{\mathrm{sp}}(E)$—as well as $P_x^{\mathrm{sp}}(E)$—changes sign if the rotation angle of the electric field vector out of the incidence plane changes sign, i.e. in the present case goes from $\pi/4$ to $-\pi/4$.

3.3. Photoemission by circular polarized light

We first briefly address the photoemission intensity. At normal incidence, circular polarized light produces the same spectra as s-polarized light, which is obvious from symmetry considerations as well as from equations (9) and (12) with $\vartheta = 0^\circ$. At off-normal incidence, the intensity is the same as for sp-polarized light (linear with $\boldsymbol{E}$ at 45° out of the incidence

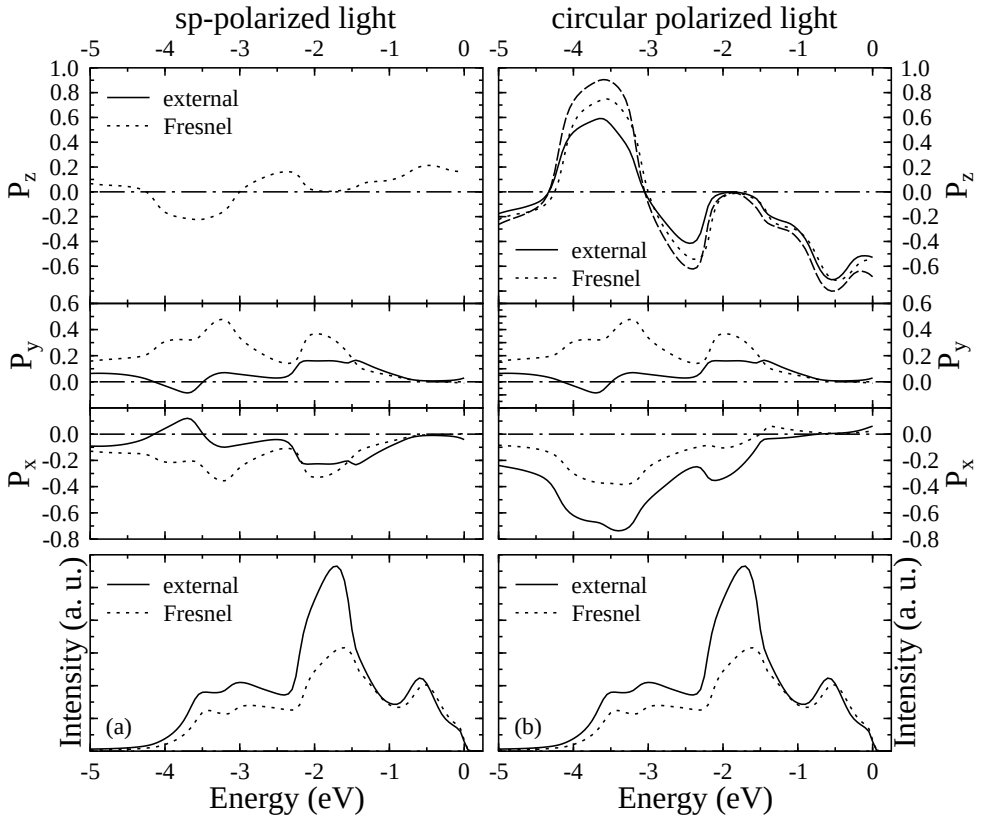

Figure 5. Normal photoemission from Pt(001) by 21.22 eV light incident in the xz-plane with $\vartheta = 45^\circ$. (a) For sp-polarized light, i.e. linearly polarized light with the incident $\boldsymbol{E}$ rotated by $\pi/4$ out of the incidence plane: intensity and spin-polarization components P_x (along [100]-direction), P_y (along [010]) and P_z (along [001]) as calculated using the external electric field (solid lines) and the Fresnel field (dotted lines). Note that P_z is zero using the external field. (b) As (a), but for positive-helicity circular polarized light incident at $\vartheta = 45^\circ$. In addition, P_z for normally incident circular polarized light is shown (dashed line in the topmost panel).

plane). This is anticipated from our analytical expressions and confirmed by the numerical results shown in the bottom panel of figure 5.

Far more interesting is the spin-polarization vector $\boldsymbol{P}$, the components of which are shown in the right-hand part of figure 5. For normal incident circular polarized light, it is completely aligned to the surface normal (z-axis). As is well known (cf e.g. [4, 5] and references therein), P_z is, for positive photon helicity, positive (negative) for emission from initial states of double-group symmetry Δ_6 (Δ_7). In particular, the $+90\%$ feature around -3.7 eV and the -70% feature around -0.7 eV are thus directly related to crossing points between initial- and final-state bands (cf panel (a) of figure 4), which are associated with peaks in the $I(\vartheta = 0^\circ)$ spectrum in panel (b) of figure 4. The $I(\vartheta = 0^\circ)$ peak at -1.5 eV arises from Δ_6 and from Δ_7 bands (so close in energy that the finite electron and hole lifetimes prevent their resolution) and is consequently associated with $P_z = 0$. Going to off-normal incidence ($\vartheta = 45^\circ$), the shape of P_z remains almost unchanged, but its magnitude is reduced due to the additional emission from states with Δ_6^1 spatial symmetry. This reduction is weaker for the curves obtained in the Fresnel approximation, which is

plausible from the smaller (real part of the) internal incidence angle.

Now consider the components of $\boldsymbol{P}$ parallel to the surface produced by circular polarized light incident at $\vartheta = 45^\circ$ in the xz-plane. As is seen from figure 5, the spectra of P_y (the component normal to the incidence plane) without and with Fresnel are the same as their counterparts obtained for sp-polarized light. This is in accordance with equation (10*b*) (with $\varphi = 0^\circ$), since the relevant factor $|E'_\parallel|^2$ is the same for circular and for sp-polarized light. In contrast, the P_x spectra differ most strongly in the external-field approximation. This is directly understandable from equations (17*a*) and (21*a*): for sp-polarized light, P_x is determined by $\mathrm{Im}(M_6^{(1)} M_6^{(5)\star})$, whereas for circular polarized light it is determined by $\mathrm{Re}(M_6^{(1)} M_6^{(5)\star})$. In the Fresnel approximation, the P_x-expression equation (10*a*) involves both of these matrix element terms and depends on the electric field via $E'_\parallel E'^{\star}_\perp$. Since $E'_\perp$ for circular polarized light differs from that for sp-polarized light by a factor of i, P_x should in general be different for the two polarization types, but less strongly so than in the external-field approximation. This is also qualitatively plausible, since for both circular and sp-polarized light the internal field is elliptically polarized, i.e. has a linear and a circular polarized part. For circular polarized incident light, the Fresnel correction is seen (cf figure 5) to reduce P_x over a wide energy range by about a factor of two. Around -1.7 eV, where the main intensity peak is located, it is even reduced from -30% to only -10%. It is interesting to note that at this peak energy sp-polarized light produces P_x values of about -20% without Fresnel and -30% with Fresnel.

Since the dielectric function is strongly energy dependent (cf [21]), it remains to be investigated how Fresnel quantitatively affects the photo-electron spin polarization vector at other photon energies.

4. Conclusion

Spin-polarized photoemission normal to (001) surfaces of non-magnetic cubic solids has, within a relativistic one-step model, been approached in a twofold way: analytically and numerically. We analytically derived explicit formulae for both the intensity and the spin-polarization vector of the photo-electrons produced by off-normally incident light in a general state of polarization. The optical response of the solid has been approximately included by employing the classical internal field according to Fresnel's formulae. The connection with spin-polarized photoemission from atoms has been considered qualitatively. In particular the orientation of the spin-polarization vector differs in the case of a solid surface due to a spin-polarization effect for off-normally incident p-polarized light. Our analytical results are fully confirmed and quantitatively illustrated by the results of numerical calculations, which we performed for Pt(001) using a relativistic Green function method.

Qualitatively novel and in fact sizeable spin-polarization effects are, as a consequence of spin–orbit coupling in the initial states, predicted for off-normally incident linear polarized light with the electric field vector rotated out of the incidence plane (which we refer to as sp-polarized light): for both the external field and the Fresnel field there is a spin-polarization component, which is parallel to the surface and to the incidence plane; further, the Fresnel field leads to a spin-polarization component normal to the surface, similar to the one obtained for circular polarized incident light.

In all cases considered (except for s-polarized light and normally incident light), the Fresnel approximation was found—in addition to significantly affecting ratios of intensity peaks—to rather drastically modify the spin-polarization vector. This raises the question of whether an improvement of the treatment of the optical response of the metal would entail

further significant changes. We therefore performed analogous calculations using, as a fairly simple approximation 'beyond Fresnel', the so-called hydrodynamical model of metal optics [24]. In contrast to the pronounced influence found for semiconductors by Schattke's group [25], we obtained intensity and spin-polarization spectra almost identical to the ones in the Fresnel approximation. This is understandable from the fact that our photon energy 21.22 eV is well above plasmon frequencies in Pt and the induced longitudinal electric field is consequently very small.

We hope that our theoretical spin polarization results, in particular those for sp-polarized light, will stimulate their experimental verification. From the detailed comparison of calculated and measured spectra one can also expect an answer to the question of whether and under which conditions a more sophisticated treatment of the optical response is required in photoemission theory from metals.

Finally, we would like to point out the relevance of this study on non-magnetic systems for photoemission from ferromagnets. From previous investigations (cf [1] and references therein) it is clear that the spin–orbit-induced spin-polarization components, which we predicted, especially P_x and P_z for sp-polarized light, will give rise to magnetic dichroism if the magnetization direction is aligned to them.

Acknowledgment

This work has been supported by the Bundesministerium für Bildung, Wissenschaft, Forschung und Technologie, contract No 05621PGA.

References

[1] Feder R and Henk J 1996 *Spin–Orbit Influenced Spectroscopies of Magnetic Solids (Springer Lecture Notes in Physics 466)* ed H Ebert and G Schütz (Berlin: Springer) p 85
[2] Kuch W, Dittschar A, Meinel K, Zharnikow M, Schneider C M, Kirschner J, Henk J and Feder R 1996 *Phys. Rev.* B **53** 11 621
[3] Fanelsa A, Kisker E, Henk J and Feder R 1996 *Phys. Rev.* B **54** 2922
[4] Schneider C M and Kirschner J 1996 *Crit. Rev. Solid State Mater. Sci.* **20** 179
[5] Feder R (ed) 1985 *Polarized Electrons in Surface Physics (Advanced Series in Surface Science)* (Singapore: World Scientific)
[6] Heinzmann U 1990 *Photoemission and Absorption Spectroscopy of Solids and Interfaces with Synchrotron Radiation* ed M Campagna and R Rosei (Amsterdam: North-Holland)
[7] Kessler J 1985 *Polarized Electrons* vol 1 of *Springer Series on Atoms and Plasmas* 2nd edn (Berlin: Springer)
[8] Tamura E, Piepke W and Feder R 1987 *Phys. Rev. Lett.* **59** 934
[9] Schmiedeskamp B, Vogt B and Heinzmann U 1988 *Phys. Rev. Lett.* **60** 651
[10] Tamura E and Feder R 1991 *Solid State Commun.* **79** 989
[11] Tamura E and Feder R 1991 *Europhys. Lett.* **16** 695
[12] Schmiedeskamp B, Irmer N, David R and Heinzmann U 1991 *Appl. Phys.* A **53** 418
[13] Irmer N, Frentzen F, Schmiedeskamp B and Heinzmann U 1994 *Surf. Sci.* **307–309** 1114
[14] Henk J and Feder R 1994 *Europhys. Lett.* **28** 609
[15] Irmer N, Frentzen F, Yu S-W, Schmiedeskamp B and Heinzmann U 1996 *J. Electron. Spectrosc. Rel. Phenom.* **78** 321
[16] Scheunemann T 1993 *Diploma Thesis*, Universität Duisburg Theoretische Festkörperphysik
[17] Bonzel H P, Helms C R and Kelemen S 1975 *Phys. Rev. Lett.* **35** 1237
[18] Inui T, Tanabe Y and Onodera Y 1990 *Group Theory and Its Applications in Physics* vol 78 of *Springer Series in Solid State Sciences* 1st edn (Berlin: Springer)
[19] Jackson J D 1975 *Classical Electrodynamics* (New York: Wiley)
[20] Henk J, Scheunemann T, Halilov S V and Feder R 1996 *J. Phys.: Condens. Matter* **8** 47
[21] Weaver J H 1975 *Phys. Rev.* B **11** 1416
[22] Halilov S V, Tamura E, Gollisch H, Meinert D and Feder R 1993 *J. Phys.: Condens. Matter* **5** 3859

[23] Henk J and Feder R 1994 *J. Phys.: Condens. Matter* **6** 1913
[24] Forstmann F and Gerhardts R R 1986 *Metal Optics Near the Plasma Frequency* (Berlin: Springer)
[25] Samuelsen D, Yang A, and Schattke W 1993 *Surf. Sci.* **287** 676